Bull. Mater. Sci. (2018) 41:54
https://doi.org/10.1007/s12034-018-1570-x

One-step hydrothermal synthesis of flower-like CoS hierarchitectures for application in supercapacitors

JIA ZHU[1,2], LEI XIANG[2], DONG XI[2], YAZHOU ZHOU[1] and JUAN YANG[1,*]

[1]School of Materials Science and Engineering, Jiangsu University, Zhenjiang 212013, People's Republic of China
[2]School of Environmental and Chemical Engineering, Jiangsu University of Science and Technology, Zhenjiang 212003, People's Republic of China
*Author for correspondence (yangjuan6347@ujs.edu.cn)

MS received 26 May 2017; accepted 16 August 2017; published online 29 March 2018

Abstract. Flower-like CoS hierarchitectures were successfully synthesized through a hydrothermal route in the presence of ethylenediamine as ligand and structure-directing agent. The structure and morphology of the products were characterized by X-ray diffraction, transmission electron microscopy, field emission scanning electron microscopy and N_2 adsorption–desorption isotherm. Flower-like CoS hierarchitectures are constructed by two-dimensional CoS nanopedals interlaced and stacked with each other. When tested as electrode material for supercapacitors, the as-fabricated CoS delivers a specific capacitance of 357 F g^{-1} at 0.5 A g^{-1}. After 2000 repetitive charge–discharge cycles, there is only 12.7% loss of the original specific capacitance. The results signify that the CoS supercapacitor possesses good electrochemical performances, suggesting its potential application in supercapacitor.

Keywords. CoS hierarchitecture; hydrothermal; electrochemical; supercapacitor.

1. Introduction

With the increasing energy consumption and global warming, it is imperative to search for sustainable and alternative energy conversion and storage device. Supercapacitors, also named electrochemical capacitors (ECs), were given great attention by virtue of their ultrafast charge–discharge ability, long durability, high energy density and pollution free [1,2]. In terms of charge storage mechanism, ECs can be normally sorted into two types, pseudocapacitors relied on Faradic reactions of the modified-electrode and electrical double-layer capacitors (EDLCs) involved in charge absorption and diffusion at electrode/electrolyte interface [3]. It is well-accepted that electrochemical properties of electroactive materials greatly depend on their size, morphology and architecture. Therefore, many researchers have focussed on rational designing desirable porous structures, novel heterostructures and complicated hierarchical structures of the electrode materials to further enhance the capacitive properties [4,5]. For example, the strategy of introducing structure-directing agents or ligands was extensively employed to generate electroactive materials effectively with special structures [6–8].

Among transition metal chalcogenides, cobalt sulphide with various stoichiometric compositions, like CoS, CoS_2, Co_3S_4, Co_8S_9 were widely explored. Specifically, CoS is considered as a promising candidate for supercapacitor in terms of its high reversible redox capability as well as cost effectiveness [9–11]. Up to now, CoS electrode materials fabricated via different methods have diverse nanostructures or microstructures and exhibit attractive electrochemical properties. For example, CoS microspheres [12] were produced through benign hydrothermal route in mixed solvents. CoS nanosheets [13] electrochemically deposited on nickel foam could exhibit a high specific capacitance of 1471 F g^{-1} at 4 A g^{-1} in 1 M KOH aqueous electrolyte. Hollow CoS nanoprisms [14] were prepared by a two-step and microwave-assisted method. Despite manifold alternative synthesis ways to obtain CoS material with multiple morphologies, it still remains a challenge for seeking simple, efficient and environmental-friendly means of acquiring high-performance CoS supercapacitor.

In this work, with the assistance of ethylenediamine acting as ligand and structure-directing agent, flower-like CoS hierarchitectures with high purity and single-phase crystallinity were fabricated via a simple one-step hydrothermal approach. Scanning electron microscopy (SEM) confirmed that flower-like CoS hierarchitectures were formed by two-dimensional CoS nanopedals interlaced and stacked with each other. The as-prepared CoS hierarchitectures showed a specific capacitance of 357 F g^{-1} at a current density of 0.5 A g^{-1} as electrode material for supercapacitor. After 2000 galvanostatic charge–discharge cycles at 0.5 A g^{-1}, the specific capacitance could retain 87.3% of its original capacitive value. The resultant CoS hierarchitectures have displayed excellent electrochemical properties, thus, making it applicable for high-performance supercapacitor.

2. Experimental

2.1 *Preparation of flower-like CoS hierarchitectures*

$Co(CH_3COO)_2 \cdot 4H_2O$, thiourea, ethylenediamine and ethanol were purchased commercially from Sinapham Chemical Reagent Co. Ltd. (Shanghai, China). All materials and chemicals reagents were of analytical grade and used as-received. Flower-like CoS hierarchitectures were fabricated as follows: $Co(CH_3COO)_2 \cdot 4H_2O$ (0.3 g) and thiourea (0.181 g) were initially dissolved in distilled water (20 ml). Then, the dispersion was stirred homogeneously for 30 min. Subsequently, 300 µl ethylenediamine was added to the mixture. After being stirred vigorously for 1 h, the mixture was transferred into a 25 ml Teflon-lined autoclave for hydrothermal process at 180°C for 12 h. After cooling down to room temperature, the CoS sample was separated by filtration, rinsed and centrifuged with deionized water and absolute ethanol. The final product was obtained when vacuum dried at 60°C overnight.

2.2 *Structural and morphological characterization*

The microstructure and morphology of the obtained material were observed by SEM (Hitachi SU8020) and transmission electron microscopy (TEM, JEOL 2010) using an accelerating voltage of 200 kV. The crystal structure was analysed by powder X-ray diffraction (XRD) with CuK α radiation (Rigaku Dmax 2500 PC). The specific surface area calculated by the Brunauer–Emmett–Teller (BET) method was recorded on N_2 adsorption–desorption analyzer at 77 K (ASAP 2020).

2.3 *Electrochemical determination*

To assess the electrochemical performances of the resultant CoS material, a classical three-electrode electrochemical cell including the electrolyte of 6 M KOH aqueous solution was employed. CoS-modified electrode was prepared by combining 80 wt% of CoS material, 10 wt% carbon black and 10 wt% polytetrafluoroethylene (PTFE) binder into a slurry. The slurry was thoroughly mixed, loaded onto Ni foam (1 cm × 1 cm), and then pressed at 10 MPa. After vacuum drying at 80°C for 10 h, working electrode based on CoS-modified electrode was obtained. Platinum foil and saturated calomel electrode (SCE) acted as counter and reference electrodes, respectively. The electrochemical determinations containing cyclic voltammetry (CV), galvanostatic charge/discharge (GCD) and electrochemical impedance spectroscopy (EIS) were tested by a CHI760E electrochemical work station (Shanghai, China). Cycling performance was measured with a CT 2001A Tester (Wuhan, China). The specific capacitance by GCD measurement can be calculated from the equation given below [15]:

$$C = I\Delta t/(m\Delta V), \quad (1)$$

where C (F g^{-1}) is the specific capacitance, I (A) the constant discharging current, Δt (s) the discharge time, ΔV (V) the potential interval and m (g) the mass of electroactive material in the electrode.

3. Results and discussion

As we know, Co^{2+} tends to cooperate with carboxyl or amine ligand to form a sexadentate complex compound [16,17]. Among a variety of ligands, ethylenediamine (EDA) is a significant amine ligand for the synthesis of several functional materials [18–21]. For the growth of flower-like CoS hierarchitectures assisted by EDA ligand, a possible process can be postulated as follows. Firstly, Co^{2+} reacted with EDA to form a sexadentate complex. Meanwhile, with increasing temperature, thiourea decomposed to release S^{2-} slowly. The generated S^{2-} could gradually react with Co ion of the formed sexadentate complex to produce CoS nucleus. Consequently, the CoS crystalline grew into flower-like CoS hierarchitectures through the well-known Ostwald ripening process. During the hydrothermal process, EDA reduced the concentration of the free Co ions via effective cooperation with Co ions. Furthermore, the gradual generation of S^{2-} as the decomposition of thiourea restricted cohesion and growth of crystal. This is favourable for the production of flower-like CoS hierarchitectures.

The structure composition of as-prepared CoS powder was characterized by XRD. The XRD pattern in figure 1 shows six diffraction peaks at $2\theta = 30.6°, 35.3°, 46.9°, 54.4°, 62.6°$ and 66.6°, which unambiguously correspond to the respective (100), (101), (102), (110), (103) and (201) phase planes of CoS. All the diffraction peaks are consistent with the standard hexagonal CoS with the lattice parameters $a = b = 3.368$ Å, c = 5.17 Å (JCPDS no. 65-3418).

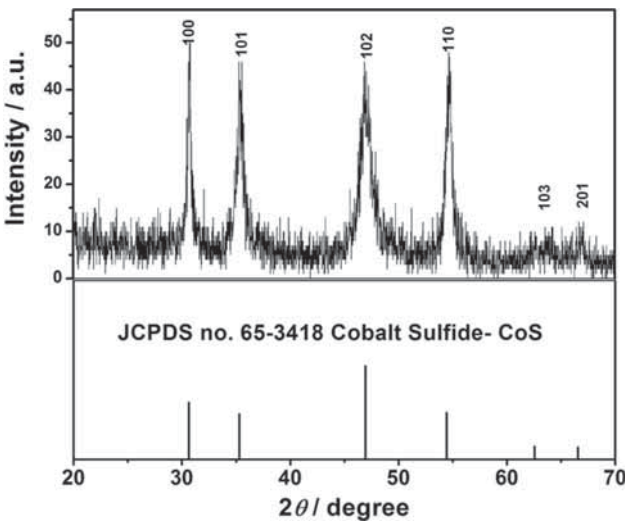

Figure 1. XRD pattern of CoS product.

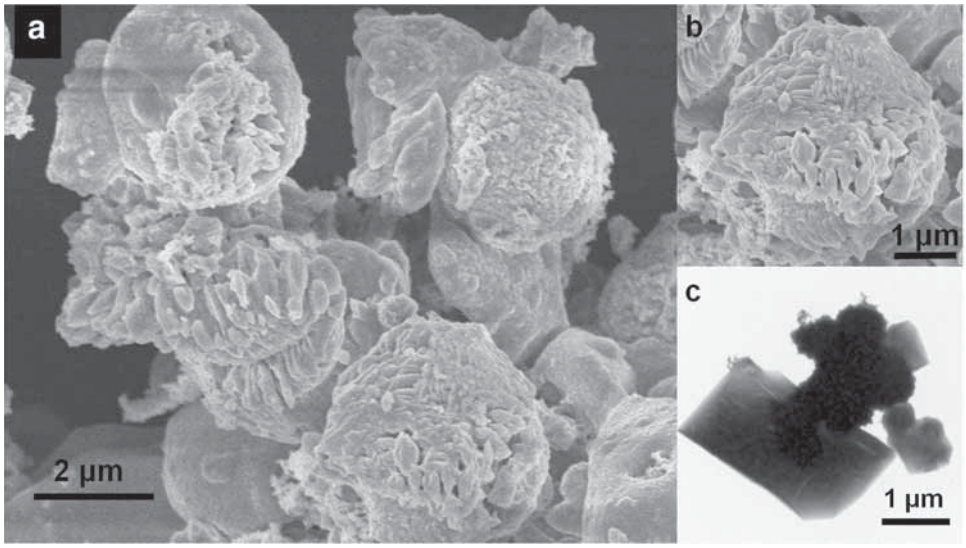

Figure 2. (**a** and **b**) SEM and (**c**) TEM images of CoS product.

No characteristic peaks from other phases were observed, implying high purity and single-phase crystallization of the sample. Additionally, the weak intensity of diffraction peaks reflects weak crystallinity of the product.

The morphology of the CoS hierarchitectures was characterized by SEM. Typical magnified SEM images shown in figure 2a and b reveal that resultant CoS product is composed of quasi flower-like microspheres with various diameters. It can be clearly noted that these flower-like CoS hierarchitectures are constructed by two-dimensional CoS nanopedals cross-linked and stacked with each other. The large particle size and flower-like microstructure result in a limited BET specific surface (figure 3). To further specify this interesting microstructure, typical TEM image of CoS material is shown in figure 2c. CoS sample exhibits densely packed clusters which are in groups of flower-like hierarchitectures. In good accordance with SEM analysis, the improved transparency under TEM observation identifies some apparent nanoplates at the surface of the quasi flower-like microspheres. This internal interlaced structure of the nanopedals could effectively maintain the long-standing existence of the architecture.

The N_2 adsorption–desorption isotherm plots of as-prepared CoS is shown in figure 3. The plot shows a representative IV isotherm with an apparent hysteresis loop starting from $P/P_0 = 0.015$. The BET surface area and total pore volume of flower-like CoS hierarchitectures are determined to be 0.176 $m^2\ g^{-1}$ and 0.03 $cm^3\ g^{-1}$, respectively. These relatively low values are an additional indication of the typical large particle size characteristics of CoS hierarchitectures.

The capacitive properties of flower-like CoS hierarchitectures were determined via CV. The detailed CVs of as-synthesized CoS at different scan rates are illustrated in figure 4a. The shapes of the CV curves based on CoS-modified electrode suggest that capacitive feature of CoS-modified electrode is distinct from that of EDLC, whose CV

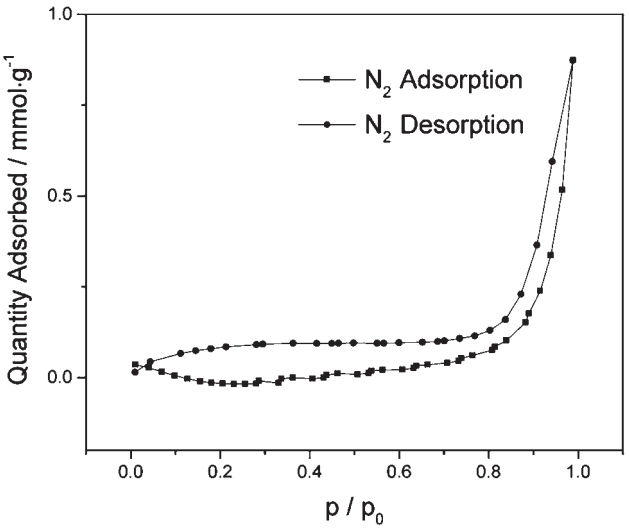

Figure 3. N_2 absorption–desorption isotherm of CoS product.

shape is similar to an ideal rectangle model [22]. Under observation, there is a pair of strong redox peaks in CV curves, demonstrating that the as-obtained CoS electrode shows typical pseudocapacitive characteristics governed by reversible Faradaic reactions occurring in the electrochemical process. According to the reported literatures [13,23], two reasonable redox reactions of the CoS electrode in alkaline electrolytes are likely to involve in the reversible conversion processes of CoS $\leftrightharpoons$ CoSOH and CoSOH $\leftrightharpoons$ CoSO. They are described as follows:

$$CoS + OH^- \leftrightharpoons CoSOH + e^-,$$

$$CoSOH + OH^- \leftrightharpoons CoSO + H_2O + e^-.$$

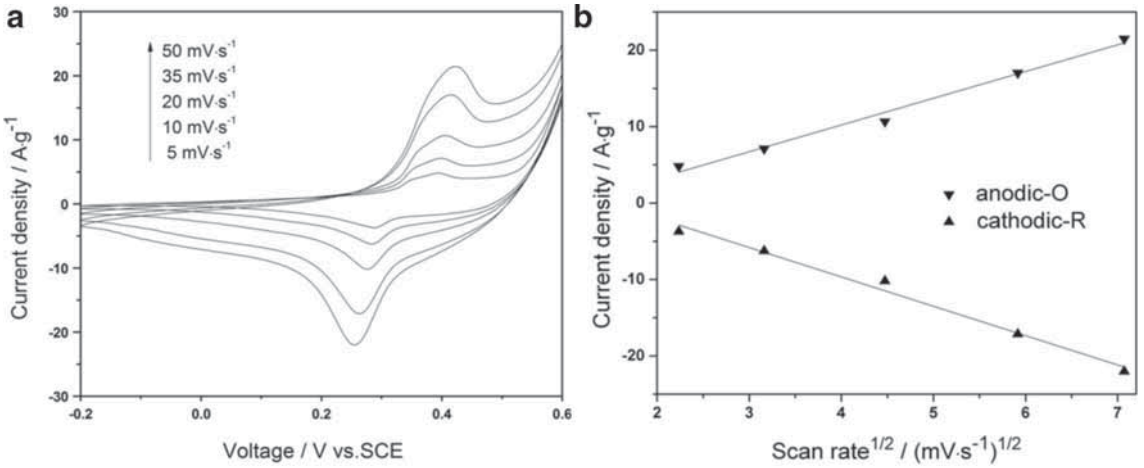

Figure 4. (**a**) CV curves of CoS-modified electrode at rising scan rates from 5 to 50 mV s^{-1}, and (**b**) plot of peak current *vs.* the square root of the scan rate of CoS electrode.

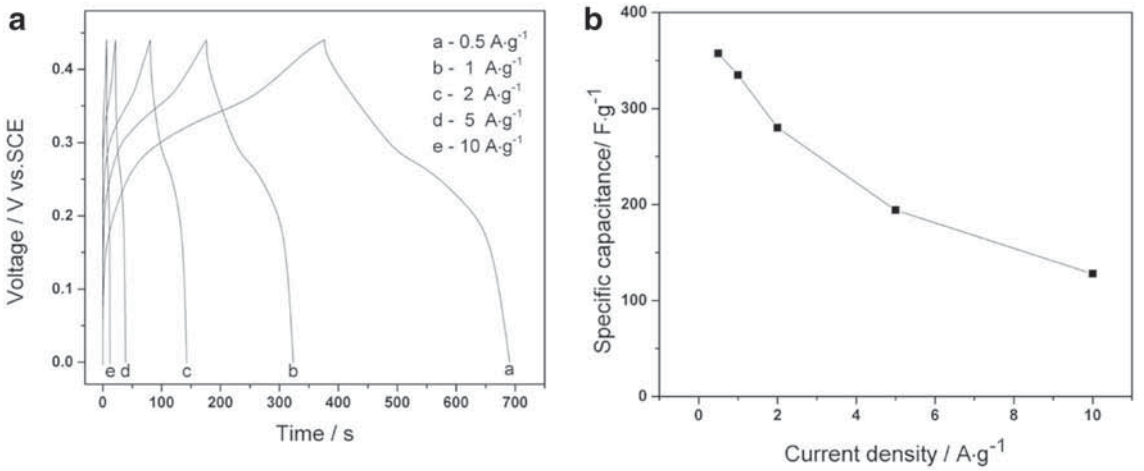

Figure 5. (**a**) GCD curves of CoS electrode at different current densities from 0.5 to 10 A g^{-1}, and (**b**) specific capacitances of CoS electrode at different current densities.

Upon an increase in scan rate, the potential of anodic and cathodic peaks move slightly to more positive and negative directions separately. This occurs because the internal diffusion resistance in the pseudoactive electrode material increases with the augmentation of scan rate [23,24]. Also the peak current densities (I_P) rise by enlarging the scan rate (V). The phenomenon may be on account of the limited ion diffusion rate failing to neutralize electronic within Faradic reactions [25]. Originated from the CV data, figure 4b gives a fine linearity between oxidation and reduction of I_P against $V^{1/2}$. As classical Sevick equation expresses [26], in semi-infinite diffusion process governed CV in liquid electrolytes, I_P *vs.* $V^{1/2}$ is a linear relationship for a kinetically plain redox reaction regardless of the scan rate. These results provide a confirmation that the diffusion process of hydroxyl ions controls the rate of redox reactions on the resulting CoS electrode.

Figure 5a presents GCD curves of CoS product at diverse current densities. During charge/discharge process, a distinct plateau region and a nonlinear relationship of potential *vs.* time appear in GCD curves, suggesting a typical pseudocapacitance characteristic deriving from the Faradic reaction between electrode and electrolyte. This analysis agrees well with the result from the CV curves. Moreover, GCD configurations display high symmetry at different current densities, illustrating remarkable pseudocapacitive behaviours and good reversible Faradic reaction capability. Based on specific capacitance calculation equation, the specific capacitance of CoS product is determined to be 358, 335, 280, 194 and 128 F g^{-1} when the current density is 0.5, 1, 2, 5 and 10 A g^{-1}, respectively (figure 5b). These values of specific capacitance are considered relatively high for pseudocapacitive performance, especially in view of the limited BET surface area (~0.176 m^2 g^{-1}). It can be ascribed to synergic effects combining metallic compound intrinsic nature and flower-like hierarchitectures microstructure. The electrode only offers 128 F g^{-1} at 10 A g^{-1}, maintaining 35% specific capacitance

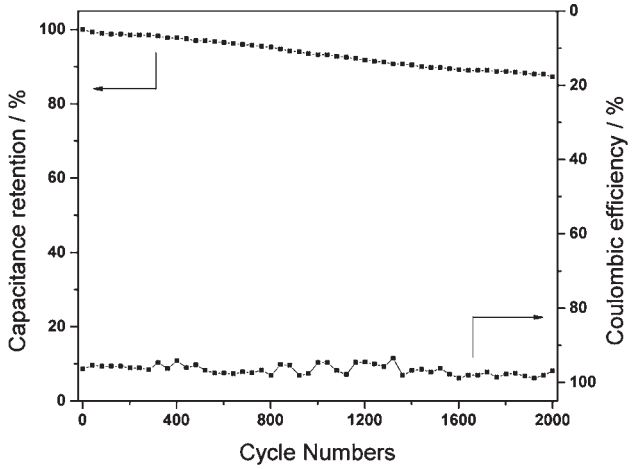

Figure 6. Cycling performance and Coulombic efficiency of CoS electrode at 0.5 A g^{-1}.

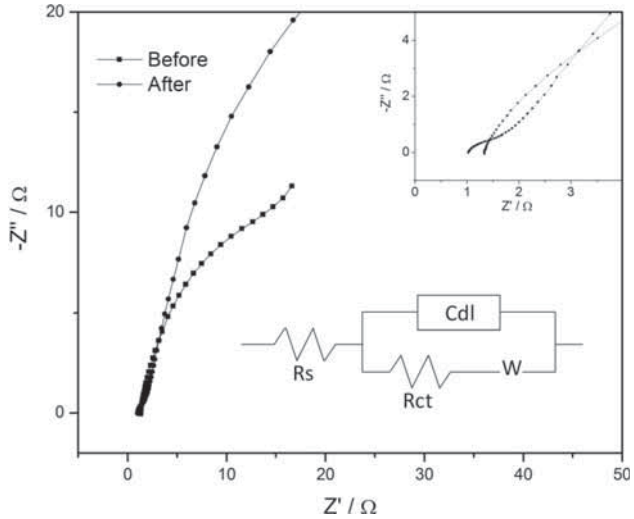

Figure 7. Nyquist plots for CoS electrode before and after cycling. The inset is the magnified plots in high frequency region and the equivalent circuit simulated the Nyquist plots.

value at 0.5 A g^{-1}. Notably, as current density varies from 0.5 to 10 A g^{-1}, the specific capacitance displays a reduction probably owing to the insufficiency of redox reaction time at high discharging rate. It is proposed that at high current densities, the fast current accumulating process restricts ion and electron transmission rates, and thus, hinders full access of active sites on the electrode and redox actions between the electrode and electrolyte [27].

To examine the charge–discharge cycling stability of CoS-modified electrode, GCD cycles were undertaken at 0.5 A g^{-1}. The specific capacitance retention and corresponding Coulombic efficiency (η) [28] for 2000 consecutive cycles are shown in figure 6. The specific capacitance retention shows gradual decrease and preserves 87.3% of the initial value after being cycled 2000 times. Additionally, η is also called charge–discharge efficiency, retains >95% during the whole charge–discharge process, demonstrating full activation and a high efficiency of the CoS-modified electrode. These results verify that the CoS-based electrode exhibits superiority for supercapacitor with excellent cycling stability and high efficiency.

For further understanding the detailed electrochemical performance of the as-prepared CoS electrode, EIS measurements were undertaken at open circuit potential with a fixed amplitude of 5 mV in the frequency range of 0.1–10 kHz. The Nyquist plots (figure 7) of CoS-modified electrode before and after cycling are compared. Both EIS spectra share a similar shape and exhibit a small depressed semicircle arch at high frequency region and a sloped line at low frequency region. According to the equivalent circuit (inset of figure 7), the x-axis intercept in high frequency region is a representation of solution resistance (R_S), combining inherent electrode resistance and contact resistance at electrolyte/electrode interfaces. Accordingly, the R_S values of CoS-modified electrode before and after cycling are 1.38 and 1.03 Ω, respectively. In high-medium frequency region, the diameter of the semicircle arch along x-axis corresponds to charge-transfer resistance (R_{ct}), which determines the response rate of electrode material in electrolyte. As observed from the magnified ESI data, after cycling, CoS-modified electrode possesses a little smaller R_{ct}, revealing a bit higher electric conductivity. A plausible explanation can be that after cycling, sufficient electrolyte permeation and wetting within the interior of electrode favours the rapid transportation of electrons, thus, reducing R_{ct} and enhancing electric conductivity [29,30]. In low frequency range, the slope of the straight line represents Warburg resistance (W) associating with ions diffusion from the electrolyte to the electrode interface. After cycling, the higher slope of the straight line demonstrates faster ion transfer rates between electrode and electrolyte. Furthermore, the nearly vertical linear part in the EIS spectra suggests that as-obtained CoS electrode for supercapacitor is an ideal capacitor model [31]. Overall, the results manifest that CoS-modified electrode after cycling has desirable fast ions transport rates and charge-transfer kinetics; thus, presenting excellent capacitance properties [32].

4. Conclusions

Flower-like CoS hierarchitectures with high purity were successfully fabricated by a one-step hydrothermal method with the help of EDA as ligand and structure-directing agent. Two-dimensional CoS nanopedals interlaced and stacked with each other to form flower-like CoS hierarchitectures. When utilized as electrode material for supercapacitor, the CoS hierarchitectures show typical pseudocapacitive features and exhibit excellent cycling durability. The specific capacitance of CoS hierarchitectures reaches 357 F g^{-1} at 0.5 A g^{-1}. After 2000 GCD cycles at 0.5 A g^{-1}, the specific capacitance remains 87.3% of its initial value. This CoS active material with novel

hierarchitectures may have other potential applications in lithium–sulphur batteries, sodium-ion batteries and oxygen evolution reaction catalysts.

Acknowledgements

This work was financially supported by Natural Science Foundation of China (No. 51672112).

References

[1] Sharma P and Bhatti T S 2010 *Energy Convers. Manag.* **51** 2901
[2] Simon P and Gogotsi Y 2008 *Nat. Mater.* **7** 845
[3] Winter M and Brodd R J 2004 *Chem. Rev.* **104** 4245
[4] Yang Q M, Zhao L, Xu X, Xu L and Luo Y Z 2011 *Nat. Commun.* **2** 381
[5] Huang M, Mi K, Zhang J H, Liu H L, Yu T T, Yuan A H *et al* 2017 *J. Mater. Chem. A* **5** 266
[6] Maqbool Q, Singh C, Jash P, Paul A and Srivastava A 2017 *Chem. Eur. J.* **23** 4216
[7] Fan H L, Niu R T, Duan J Q, Liu W and Shen W Z 2016 *ACS Appl. Mat. Interf.* **8** 19475
[8] Barkaoui S, Haddaoui M, Dhaouadi H, Raouafi N and Touati F 2015 *J. Solid State Chem.* **228** 226
[9] Tao F, Zhao Y Q, Zhang G Q and Li H L 2007 *Electrochem. Commun.* **9** 1282
[10] Chiu J M, Lin L Y, Yeh P H, Lai C Y, Teng K, Tu C C *et al* 2015 *RSC Adv.* **5** 83383
[11] Ranaweera C K, Wang Z, Alqurashi E, Kahol P K, Dvomic P R, Gupta B K *et al* 2016 *J. Mater. Chem. A* **4** 9014
[12] Justin P and Rao G R 2010 *Int. J. Hydrog. Energy* **35** 9709
[13] Lin J Y and Chou S W 2013 *RSC Adv.* **3** 2043
[14] You B, Jiang N, Sheng M L and Sun Y J 2015 *Chem. Commun.* **51** 4252
[15] Xu B, Pan L and Zhu Q Y 2016 *J. Mater. Eng. Perform.* **25** 1117
[16] Couldwell M C, House D A and Penfold B R 1975 *Inorg. Chim. Acta* **13** 61
[17] Herak B R, Prelesnik B and Kristanovic I 1978 *Acta Cryst.* **34** 91
[18] Feng X W, Chen H and Jiang F 2017 *J. Colloid Interf. Sci.* **494** 32
[19] Caceres M, Lobato A, Mendoza N J and Baonza V G 2016 *Phys. Chem. Chem. Phys.* **18** 26192
[20] Parambadath S, Mathew A and Ha C S 2015 *Micropor. Mesopor. Mater.* **215** 67
[21] Ramkumar J, Ananthkumar S and Babu S M 2014 *Sol. Energy Mater. Sol. Cells* **106** 177
[22] Xing J C, Zhu Y L, Zhou Q W, Zheng X D and Jiao Q J 2014 *Electrochim. Acta* **136** 550
[23] Zhang C, Chen Q and Zhan H 2016 *ACS Appl. Mater. Interf.* **8** 22977
[24] Jiang C, Zhao B, Cheng J Y, Li J Q, Zhang H J, Tang Z H *et al* 2015 *Electrochim. Acta* **173** 399
[25] Lee J W, Ahn T, Soundararajan D, Ko J M and Kim J D 2011 *Chem. Commun.* **47** 6305
[26] Liu B, Yuan H, Zhang Y, Zhou Z and Song D 1999 *J. Power Sour.* **79** 277
[27] Zhang X, Miao W, Li C, Sun X Z, Wang K and Ma Y W 2015 *Mater. Res. Bull.* **71** 111
[28] Ingole R S and Lokhande B J 2016 *Bull. Mater. Sci.* **39** 1603
[29] Nguyen V H and Shim J J 2015 *Electrochim. Acta* **166** 302
[30] Liu G J, Wang B, Wang L, Liu T F, Gao T T and Wang D L 2016 *RSC Adv.* **6** 54076
[31] Zhang Q F, Xu C M and Lu B G 2014 *Electrochim. Acta* **132** 180
[32] Zhang Y W, Tian J Q, Li H Y, Wang L, Qin X Y, Asiri A M *et al* 2012 *Langmuir* **28** 12893